Research in Astron. Astrophys. **2010** Vol. **10** No. **7**, 696–706
http://www.raa-journal.org *http://www.iop.org/journals/raa*

Research in Astronomy and Astrophysics

Statistical study of EUV and X-ray transient brightenings *

Jing-Wei Li and Hui Li

Purple Mountain Observatory, Chinese Academy of Sciences, Nanjing 210008, China;
nj.lihui@pmo.ac.cn; ljwmr@163.com

Received 2010 February 10; accepted 2010 April 20

Abstract Using the visual inspection and base difference method and data from the X-ray Telescope (XRT) onboard *Hinode* and TRACE with improved spatial and temporal resolution, we selected 48 X-ray transient brightenings (XTBs) and 237 EUV transient brightenings (ETBs) to study the connection between these two types of transient brightenings (TBs). These ETBs and XTBs have smaller areas (8.42 Mm^2 and 36.3 Mm^2, respectively, on average) and shorter durations (9.0 min and 6.9 min, respectively, on average) than previous studies. These XTBs show three types of morphological structure: point-like, single-loop and multiple-loop. We find only 20% of the ETBs have corresponding XTBs while the other 80% have no X-ray signatures at all. This is presumably due to the small amount of released energy, which is not enough to heat the plasma to coronal temperatures which produce X-ray emission rather than being due to the limitation of spatial resolution and temperature sensitivity of the X-ray instrument. These small ETBs may significantly contribute to the coronal heating.

Key words: Sun: X-rays, gamma rays — Sun: UV radiation — Sun: corona

1 INTRODUCTION

Transient brightenings (TBs) on the Sun refer to events that show small-scale enhancements in their brightness in a short time scale (a few minutes to tens of minutes), which, based on the observation waveband, are classified as X-ray transient brightenings (XTBs) and extreme-ultraviolet (EUV) transient brightenings (ETBs).

XTBs have been observed in active regions and X-ray bright points (XBPs) (Shimizu 2004). XBPs are small-scale soft X-ray (SXR) phenomena, which can occur everywhere in the quiet Sun or coronal hole region and last about 8 h (Golub et al. 1974) to 20 h (Zhang et al. 2001). XTBs are generally located in three types of regions depending on their locations: around the outer boundary of the well-developed sunspots, in coronal bundles connecting the leading and following magnetic polarity regions, and in and around emerging flux regions (EFRs) where successive emergences of magnetic flux are significant (Shimizu 2004).

Shimizu et al. (1994) classified XTBs into three morphological categories: point-like brightenings, brightenings of a single loop, and simultaneous brightenings of multiple loops. Based on the observations from the soft X-ray telescope (SXT; Tsuneta et al. 1991) onboard the *Yohkoh* satellite (Ogawara et al. 1991), XTBs of compact coronal loops have been found in active regions (Shimizu

* Supported by the National Natural Science Foundation of China.

et al. 1992, 1994). XTBs detected in active regions are called active region transient brightenings (ARTBs; Shimizu et al. 1992). Shimizu et al. (1994) and Shimizu (1995) studied ARTB's morphology, energy, temperature, emission measure, duration and area. They found that ARTBs occur on average once every 3 min in "active" active regions and down to about once per hour in relatively "quieter" active regions. This suggests that the XTBs are a very common phenomenon in active regions and that the magnetic loops in active regions are far from static (Shimizu et al. 1992). The duration of XTBs varies from 2 to 7 min (Shimizu 1995).

Berghmans et al. (1998) used data from the Extreme-ultraviolet Imaging Telescope (EIT; Delaboudiniére et al. 1995) onboard the Solar and Heliospheric Observatory (*SOHO*; Domingoet al. 1995) to study quiet Sun ETBs. ETBs are distributed over the whole field of view (FOV), but the strongest events are mainly concentrated in the core of an active region surrounding the main sunspot of the region (Berghmans et al. 1999). Berghmans & Clette (1999) studied the active region ETBs and found that they had similar characteristics to the ARTBs seen in soft X-rays with an area of 10–100 Mm^2 and a duration of 1–15 min.

With the improved spatial and temporal resolution of the Transition Region and Coronal Explorer (TRACE; Handy et al. 1999), more coronal brightenings with smaller areas were detected. After studying 41 soft X-ray brightenings and 373 EUV brightenings in the NOAA 8218 active region observed simultaneously with *Yohkoh*/SXT, *SOHO*/EIT and TRACE, Berghmans et al. (2001) found that the strongest brightenings on the EIT images are indeed the EUV counterparts of the XTB seen with SXT. Weaker brightenings observed with EIT often do not have an X-ray counterpart. The strongest XTBs belong to GOES (Geostationary Operational Environmental Satellites) A and B class flares. There is, however, no one to one correspondence, as the flares identified by GOES seem to consist of several XTBs which are spatially separated. This led to the concept of sympathetic XTBs that collectively form a GOES flare. Analogously, most of these stronger XTBs detected with SXT often correspond to several ETBs seen with EIT and TRACE.

It was reported that a lot of tiny TRACE ETBs have no accompanying *Yohkoh*/SXT TBs (Berghmans et al. 2001). This is presumably due to the lower spatial resolution of *Yohkoh*/SXT with respect to the X-ray Telescope (XRT; Golub et al. 2007) on the *Hinode* satellite and higher responding temperature (*Yohkoh*/SXT is sensitive to the plasma higher than 2 MK) (Li et al. 2007). At the same time, many of the weaker ETBs have no soft X-ray counterpart, possibly because they have a smaller amount of energy, which is not enough to heat the plasma to beyond 2×10^6 K (Berghmans et al. 2001).

The XRT has higher spatial and temporal resolution, wider temperature coverage, and a wider FOV than SXT. In this paper, we used the high-resolution images acquired with the *Hinode*/XRT ($1.032''$ pixel^{-1}) and TRACE ($0.5''$ pixel^{-1}) in high cadence mode to statistically study XTBs and ETBs in terms of geometry/topology, areas and evolution during solar minimum.

This paper is organized as follows: in Section 2, we introduce the observation and data reduction, and give our results in Section 3, while the discussions and conclusions are presented in the last section of the paper (Sect. 4).

2 OBSERVATION AND DATA REDUCTION

Data used in this paper were obtained on 2007 May 11, 13, 16 and July 12 with *Hinode*/XRT (thin-Al/poly, thin-Al/mesh and G-band) and TRACE (171 Å and white light). The thin Aluminum Poly (thin-Al/poly) and thin Aluminum Mesh (thin-Al/mesh) filters are sensitive to a temperature range of $\log T \approx 5.5-8.0$ with the peak sensitivity at $\log T \approx 6.9$. In the high temperature part ($\log T > 6.4$), the response of the thin-Al/mesh filter is similar to the thin-Al/poly filter but slightly less sensitive, while in the low temperature part ($\log T < 6.4$) the thin-Al/mesh filter has a better response. We select data in a time range during which XRT and TRACE have continuous observations, and both G-band XRT images and white-light TRACE images are available in order to coalign the images.

The data observed with *Hinode* and TRACE were processed using standard analysis routines ('xrt_prep.pro' and 'trace_prep.pro') integrated into the Solar SoftWare (SSW) package. It should be mentioned that the current xrt_prep.pro in SSW does not correct the flat-field. The processing includes dark-current and flat-field corrections, spike removal and normalization. Afterwards, the images obtained in the same timeframe were corrected for the differential rotation of the Sun and rotated to a reference time for coalignment.

The coalignment between *Hinode*/XRT and TRACE images were made as follows. The XRT G-band image was first re-scaled to the same pixel size as the TRACE white light image, and then cross-correlation was used to find the pixel offsets between the XRT G-band and the TRACE white light images, which were then applied to the TRACE 171 Å images. Following Shimizu et al. (2007), we coaligned XRT thin-Al/poly or thin-Al/mesh images and G-band images. After all these processes, the XRT and TRACE images were coaligned with an accuracy of $1''$–$2''$.

A significant number of the TRACE images were heavily contaminated by particle hits. As a consequence of this, we did not attempt to detect ETBs in such images. We use the visual inspection method to detect the transient brightenings, and use the base difference method to determine parameters of TBs, such as area and duration. The XTB and ETB detection process is bidirectional: search XTB in X-ray images and then look for EUV counterparts in the EUV images, and vice versa. By visual inspection, we determine the event position, and ascertain that it is of solar origin if it appeared in at least two successive images. We derive a background emission image from images obtained before and/or after the event by averaging. The area of the TBs is defined as the region where brightness exceeds the background value by a threshold value (30%) of enhancement (peak brightness minus background). The duration is defined as the maximal time range on the time profile of the brightness of a TB, during which the brightness of the TB exceeds 30% of the maximal brightness. This threshold value method may miss faint or long-lasting TBs. We also use threshold values of 20% and 10% in this paper for comparison.

3 RESULTS

3.1 Examples

Using the process described above, we selected 237 ETBs and 48 XTBs. Following Shimizu et al. (1994), these XTBs can be morphologically classified into three categories: (1) point-like XTBs (13 events), (2) single-loop XTBs (29 events), and (3) multiple-loop XTBs (simultaneous brightenings of multiple loops) (6 events) (Table 1). We present here one example for each category. Note that a corresponding background emission has been subtracted from the XRT and TRACE images shown in this paper.

Table 1 Morphological Classification of X-ray Transient Brightenings

Classification	Number	This paper (%)	Shimizu et al. (1994) (%)	Berghmans et al. (2001) (%)
Total X-ray TBs	48			
Point-like X-ray TBs	13	27	18.3	10
Single loop X-ray TBs	29	60.5	41.5	70
Multiple loop X-ray TBs	6	12.5	40.2	20

3.1.1 Point-like XTB

These kinds of XTBs generally display a compact point-like brightening patch with quick enhancement of emission and expansion of area, even though it may evolve into loop-like structure in the

late phase. Twenty seven percent of the 48 XTBs belong to this category. Figure 1 shows a point-like XTB observed around 21:16 UT on 2007 May 13. It clearly demonstrates the rapid evolution of the TB. TRACE observed this TB with a cadence of 63 s and XRT with a cadence of 60 s. The ETB started at 21:15:01 UT and lasted 3.66 min, while the XTB started at 21:15:33 UT and lasted 4.67 min. We did not derive the duration of the XTB because the XRT missed the initial brightening. The maximal area of the TB in EUV and X-ray is 32.06 Mm^2 and 61.02 Mm^2, respectively.

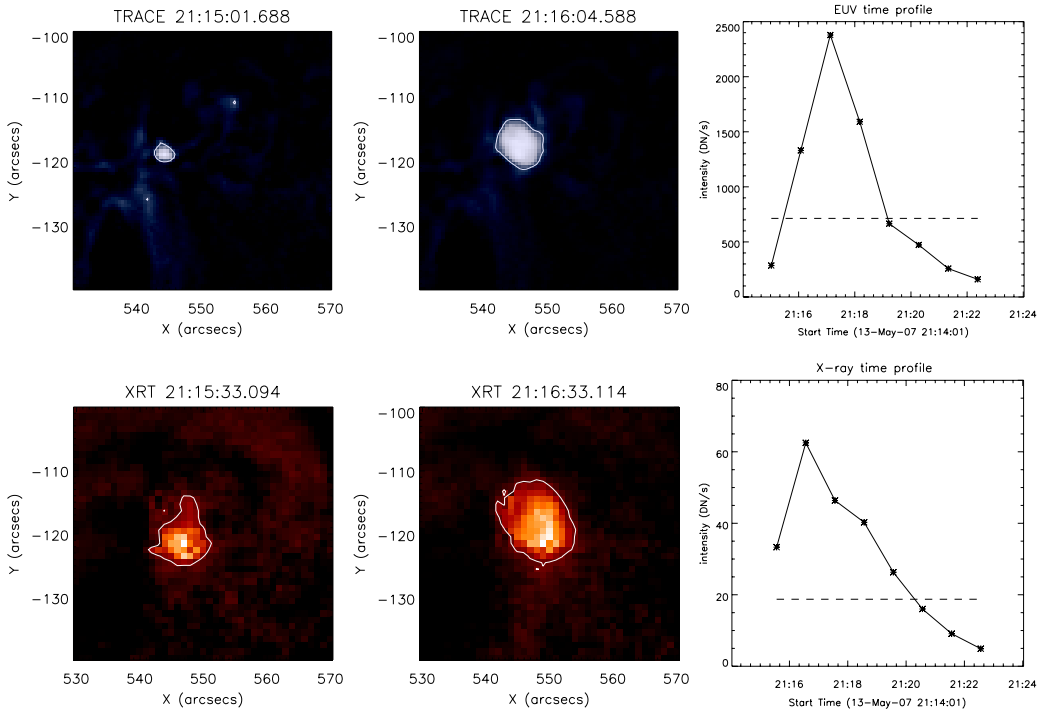

Fig. 1 A point-like XTB observed on 2007 May 13. The first row shows the EUV 171 Å images at 21:15:02 UT and 21:16:05 UT, and the EUV time profile of the TB; the second row presents the X-ray images at 21:15:33 UT and 21:16:33 UT, and the X-ray time profiles of the TB. The contour indicates the 30 % level of the remaining peak, and the dashed line marks the threshold value, which determines the duration of the TB. A background image was subtracted from the presented images. We will keep this convention throughout this paper.

3.1.2 Single-loop XTB

Single-loop XTBs generally present a loop-shaped brightening patch in the X-ray image although sometimes it may change to multiple loops as time goes on. Most of the detected XTBs (60.5%) are single-loop XTBs. An example of a single-loop XTB is shown in Figure 2. This TB was observed with XRT and TRACE around 04:38 UT on 2007 May 13. The ETB and its accompanying coronal brightening are seen simultaneously in TRACE EUV and XRT X-ray images. Again, the TRACE data were taken with a cadence of 63 s but the XRT data were taken with a cadence of 30 s. The intensity increases quickly while the area evolution is somewhat gentle compared with the above point-like XTB. The ETB lasted 5.27 min with a maximal area of 22.21 Mm^2 while the XTB lasted 3.5 min with a maximal area of 80.05 Mm^2.

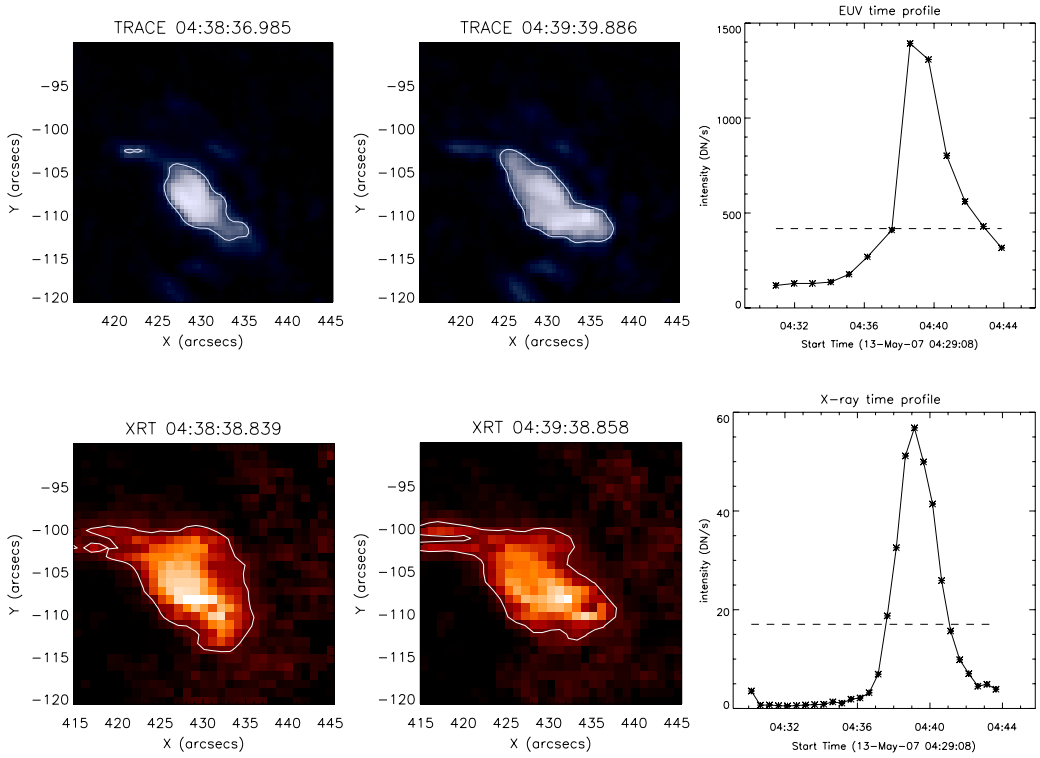

Fig. 2 Same as Fig. 1, but for a single loop XTB observed around 04:38 UT on 2007 May 13. The observation time is shown in each image.

3.1.3 Multiple-loop XTB

Multiple-loop XTBs often show multiple complicated brightening loops in both EUV and X-ray images during most of their lifetimes. Only a small part (12.5%) of the 48 studied events are multiple-loop XTBs. Due to the complicated structure, multiple-loop XTBs and their EUV counterparts commonly have larger areas than the above point-like and single-loop XTBs. Figure 3 shows the evolution and time profile of a multiple-loop XTB observed around 20:54 UT of 2007 May 13. Being the point-like XTB in Section 3.1.1, TRACE EUV images for this TB were taken with a cadence of 63 s and XRT images with a cadence of 60 s. This ETB has a duration of 3.5 min and an area of 44.28 Mm^2 while the XTB has 6.3 min and 120.36 Mm^2 respectively.

3.1.4 ETB without an XTB counterpart

Most of the ETBs detected in this study have no X-ray counterparts at all. Figure 4 is an example of this kind of ETBs occurring in an active region, which lasted 3.08 min, and we did not find any corresponding brightening signature in XRT images by the visual inspection method. Another such ETB example is given in Figure 5, which took place in a quiet Sun region and lasted 4.36 min. The time profiles of such ETBs have similar variations as the above three kinds of ETBs, all of which have accompanying XTBs.

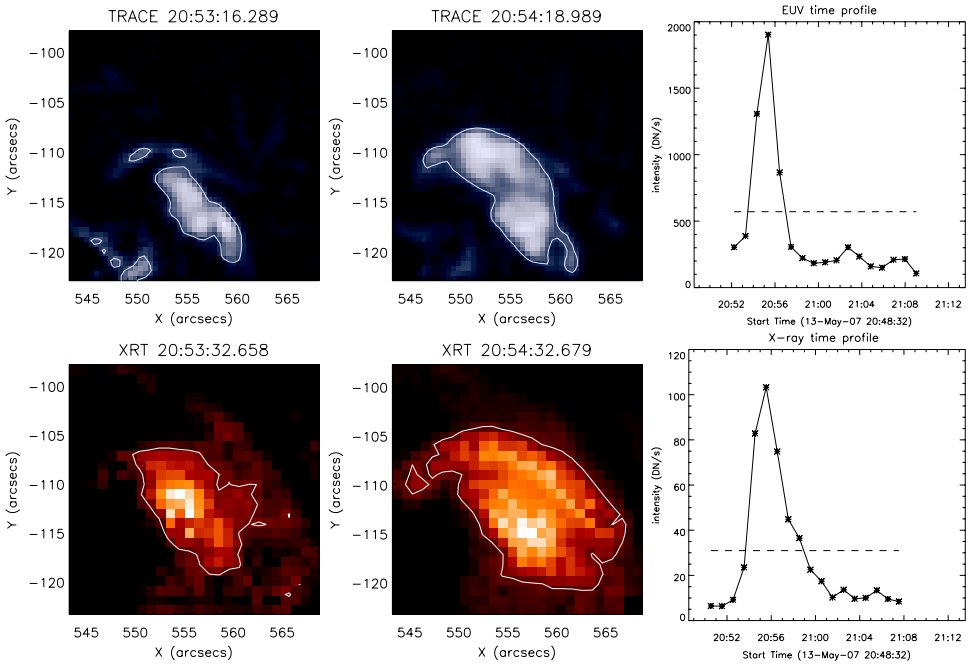

Fig. 3 Same as Fig. 1, but for a multiple loop XTB observed around 20:54 UT of 2007 May 13. The observation time is shown in each image.

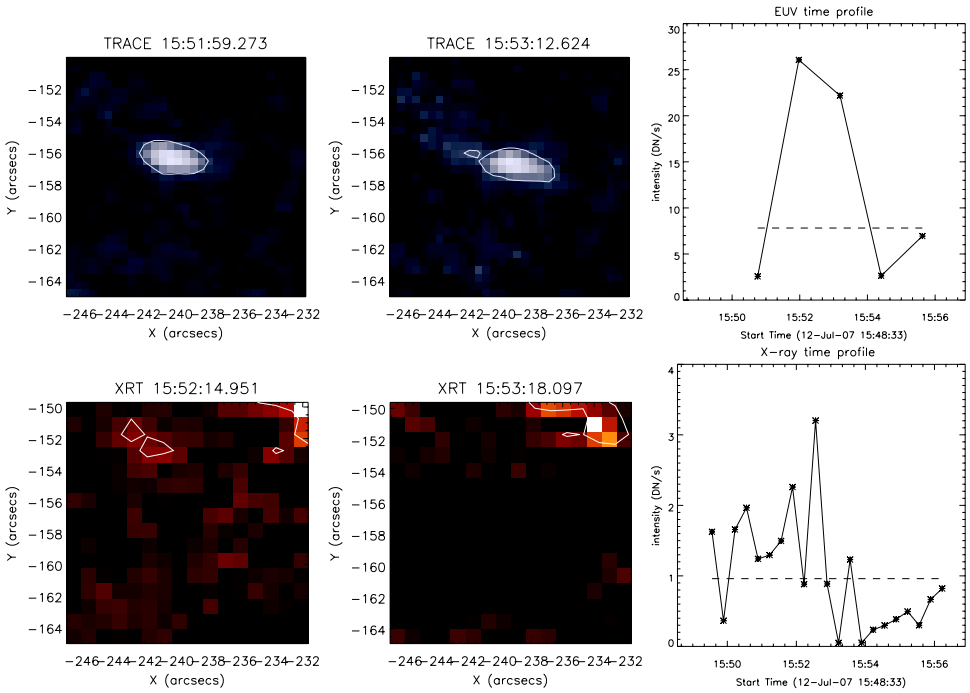

Fig. 4 Same as Fig. 1, but for an ETB in an active region without an XTB counterpart observed around 15:53 UT on 2007 July 12. The observation time is shown in each image.

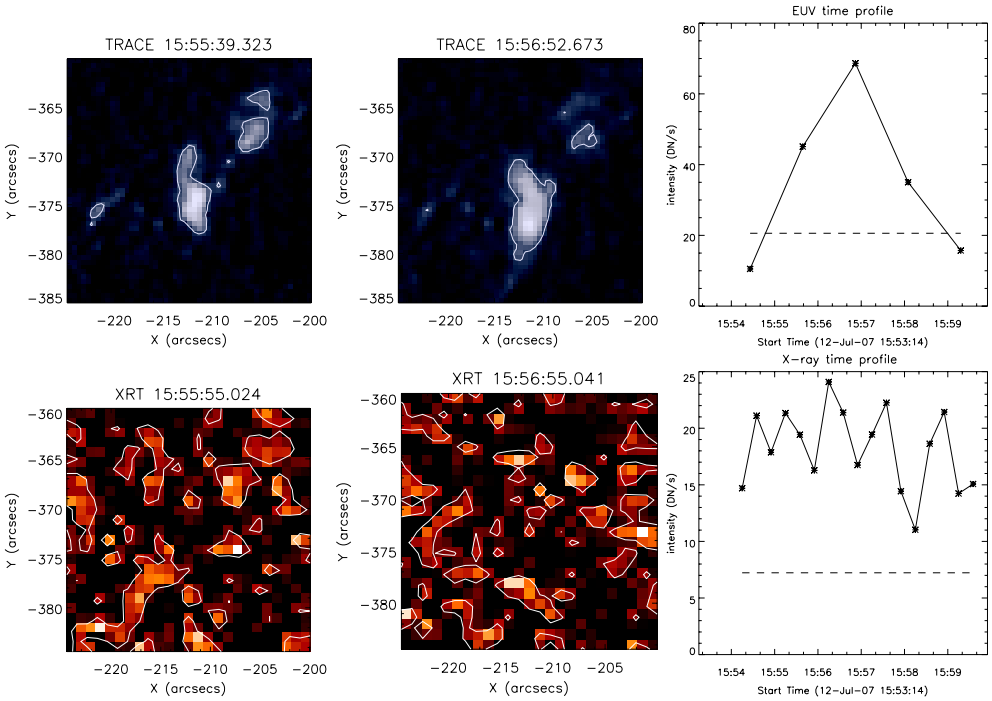

Fig. 5 Same as Fig. 1, but for an ETB in a quiet Sun region without an XTB counterpart observed around 15:57 UT on 2007 July 12. The observation time is shown in each image.

3.2 Statistical Results

There are 237 ETBs and 48 XTBs selected in this paper. All the XTBs have their EUV counterparts while only a small part (∼20%) of the ETBs have corresponding XTBs.

We calculated the durations and areas of these ETBs and XTBs using the default threshold of 30%, which is smaller than that used in Shimizu (1995), and list some statistical parameters in Table 2. We also give previous values from other authors in this table for comparison. The durations of the 48 XTBs are 1.57– 14 min with an exception of one which was about 20 min. The mean value of the duration is 6.9 min and the median value is 6.45 min. The XTBs have an average area of 36.3 Mm^2, which varies in the range of 6.16–120 Mm^2. These values, on average, are smaller than previous values obtained by other authors for ARTBs. Shimizu (1995) obtained 2–7 min durations and 10–280 Mm^2 areas. Berghmans & Clette (1999) obtained 1–17 min durations for XTBs with an average of 5.1 min and an average area of 145 Mm^2 (Table 2).

The durations of the 237 ETBs are in the range of 2.6–24 min with an average of 9.0 min and a median value of 7.76 min, and the areas are in the range 1.45–54.9 Mm^2 with an average of 8.42 Mm^2. Berghmans & Clette (1999) obtained 1–15 min durations for ETBs with an average of 7.8 min, and 10–100 Mm^2 areas with 79 Mm^2 as the mean value, which are larger than values obtained in this study.

We display the distribution of locations of studied TBs on the solar disk in Figure 6. Squares in the figure represent ETBs having accompanying XTBs, while asterisks are for those without accompanying XTBs. The figure seems to show that ETBs are mainly located in the low-altitude area. This is just because we did not use data taken in the high-altitude region. Actually, ETBs have no preferable altitude or longitude ranges no matter whether they have corresponding XTBs or not.

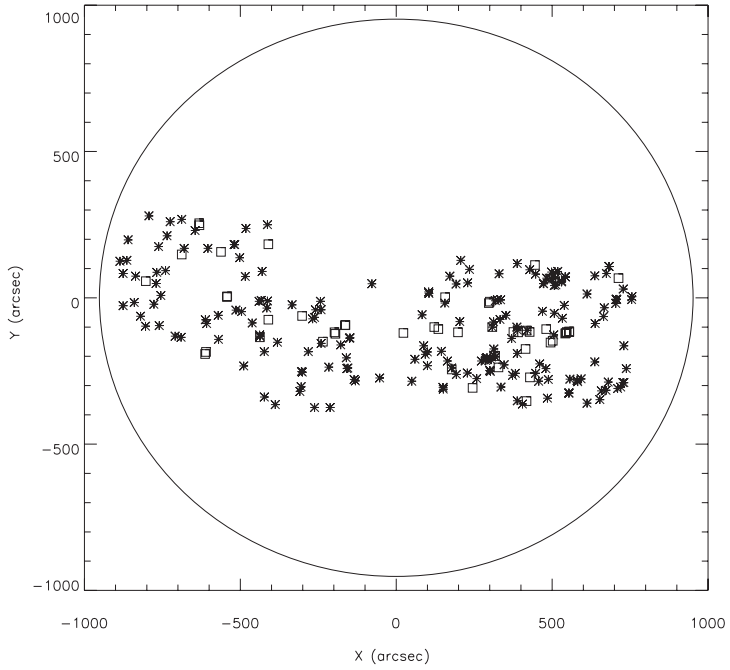

Fig. 6 Distribution of the studied ETBs on the solar disk. Squares represent ETBs having accompanying XTBs, while asterisks are for those without accompanying XTBs.

Table 2 Duration and Area of ETBs and XTBs (Threshold: 30%)

Event	Number	Duration (min)		Area (Mm^2)	
		range	average	range	average
ETB (all)	237	2.6–24	9.0	1.45–54.9	8.42
ETB (with XTB)	48	3.5–21.5	9.95	1.84–54.9	12.67
ETB (without XTB)	189	2.6–24	8.94	1.45–22.2	7.32
XTB	48	1.57–14	6.9	6.16–120	36.3
ETB (Berghmans et al. 1999)	373(68)	1–15	7.8	10–100	79
ARTB (Shimizu 1995)		2–7		10–280?	
ARTB (Berghmans et al. 1999)	41	1–17?	5.1		145

Table 3 Duration and Area of ETBs and XTBs (Threshold: 20%)

Event	Number	Duration (min)		Area (Mm^2)	
		range	average	range	average
ETB (all)	237	3–26	9.97	1.84–70.57	12.1
ETB (with XTB)	48	5–22	10.95	2.89–70.57	18.76
ETB (without XTB)	189	3–26	9.74	1.84–32.33	10.55
XTB	48	2.5–20	8.28	10.64–162.34	48

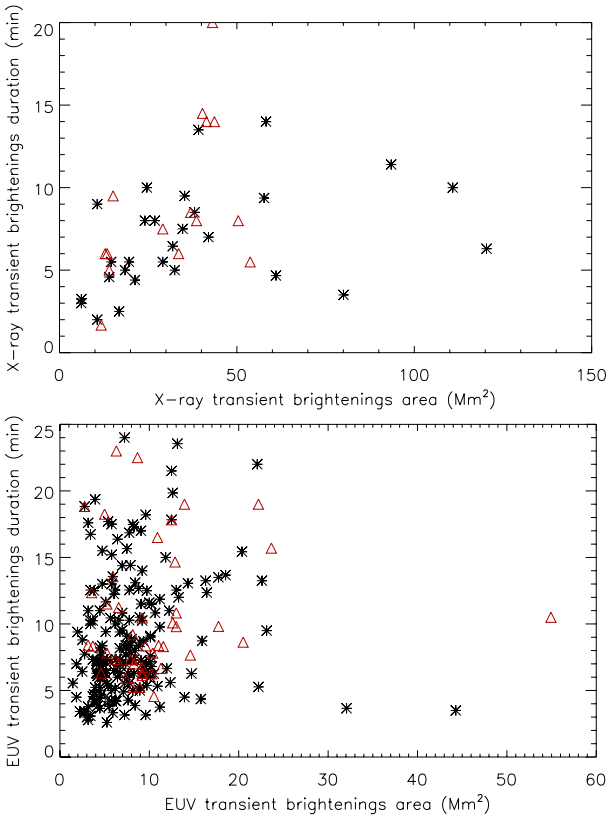

Fig. 7 Scatter map of duration versus area of the studied XTBs (*top*) and ETBs (*bottom*). Asterisks represent the events for which the durations were accurately determined while triangles are for the events whose durations were derived by extrapolation due to the absence of images in the earliest or latest phase of TBs.

Table 4 Duration and Area of ETBs and XTBs (Threshold: 10%)

Event	Number	Duration (min)		Area (Mm^2)	
		range	average	range	average
ETB (all)	237	3.65–26.7	10.42	2.63–84.1	19.37
ETB (with XTB)	48	6.3–22	11.51	5.2–84.1	28.77
ETB (without XTB)	189	3.65–26.7	10.15	2.63–53.88	17.18
XTB	48	3–20	8.7	14–207.13	66.66

To check the relation between the duration and area of the ETBs and XTBs, we plot the scatter map of duration versus area for studied ETBs and XTBs in Figure 7. In this figure, asterisks represent the events for which the durations were accurately determined while triangles are for the events whose durations were derived by extrapolation due to the absence of images in the earliest or latest phase of the TBs. Figure 7 tells us that there is a tendency for the duration to increase with increasing area for XTBs (Fig. 7, top), but this is not obvious for ETBs (Fig. 7, bottom) (the map is more scattered).

To check the validity of the default threshold value (30%), we conducted the same statistical study using thresholds of 20% and 10%, and present the results in Tables 3 and 4, respectively. From these tables, we see that, as expected, lower threshold values lead to larger areas and longer durations in the studied TBs. However, this does not change the above result, i.e., the studied ETBs and XTBs in this paper have smaller areas and longer durations compared with previous studies, even though it may overestimate the areas and durations.

4 DISCUSSION AND CONCLUSIONS

XTBs were first reported with *Yohkoh*/SXT observations about two decades ago (Shimizu et al. 1992) while ETBs were first detected with *SOHO*/EIT more than one decade ago (Berghmans et al. 1998). In this paper, using the visual inspection and base difference method and data from *Hinode*/XRT and TRACE which had improved spatial and temporal resolution, we selected 48 XTBs and 237 ETBs to study the relation between these two types of TBs frequently seen on the Sun. We found in many cases, an XTB is preceded by a smaller ETB at the same location, which still continues after the X-ray component has faded. This may indicate that the released small amount of energy first heated the low-layer plasma to EUV temperatures and then the high-layer plasma to X-ray temperatures. Among the 48 XTBs, thirteen events (27%) are point-like XTBs, twenty nine events (60.5%) are single-loop XTBs and six events (12.5%) belong to multiple-loop XTBs. We detected a larger percentage of point-like XTBs than Berghmans et al. (2001) (10%, 70%, and 20% for point-like, single-loop and multiple-loop XTBs, respectively) and Shimizu et al. (1994) (18.3%, 41.5%, and 40.2% for point-like, single-loop and multiple-loop XTBs, respectively) (cf Table 1), possibly due to the improved spatial resolution.

The ETBs seen in TRACE images last, on average, longer (9 min) but remain smaller (8.42 Mm ^{2}, on average) than XTBs seen in XRT images. These differences maybe reflect a true difference in the properties of ETBs and XTBs. Meanwhile, ETBs are spread more randomly over the FOV (they were found in both active regions and quiet Sun regions), while all of the XTBs are located in active regions and XBPs.

As Berghmans et al. (2001) reported, a lot of tiny TRACE ETBs have no X-ray counterparts. We found that only about 20% of the ETBs have corresponding XTBs, even though all XTBs have one or more ETB counterparts. It can be inferred that ETBs with X-ray counterparts are located in active regions while those without corresponding X-ray brightenings may take place in both active regions and quiet Sun regions. It seems to us that the improved resolution of the *Hinode*/XRT and its lower, wider temperature coverage with respect to *Yohkoh*/SXR does not help us to increase the percentage of ETBs that have corresponding XTBs. However, it allows us to detect XTBs with smaller areas and shorter durations (cf. Table 2).

We observed smaller ETBs than Berghmans et al. (2001). These ETBs result from a weaker energy release process, which is not enough to heat the plasma to a temperature higher than ~ 2 MK, and thus they are not visible in XRT images even with higher sensitivity to lower temperature and higher spatial resolution. These ETBs may show a scaled-down geometry of small flare loops that barely stick out of the transient region, and therefore are undetectable in X-rays. The fact that the ETBs without accompanying XTBs have smaller areas and shorter durations than the ETBs with corresponding XTBs (cf Table 2) may provide some circumstantial evidence for this result. It was estimated that the total energy supplied by XTBs and flares to heat the corona is at least a factor of 5 smaller than the heating rate required for the active region corona (Shimizu 1995). The smaller ETBs may play an important role in heating the solar corona (Berghmans et al. 1998; Berghmans & Clette 1999; Berghmans et al. 2001).

In summary, with visual inspection and a base difference method, we detected 237 ETBs from TRACE 171 Å images and 48 XTBs from *Hinode*/XRT images obtained with the thin-Al filter. These ETBs and XTBs have smaller areas and shorter durations than found in previous studies.

These XTBs show three types of structures: point-like, single-loop and multiple-loop. We find only 20% of the ETBs have corresponding XTBs while the remaining 80% have no X-ray signatures at all. This is presumably due to the small amount of released energy, which cannot heat the plasma to a temperature which produces X-ray emission rather than due to the limitation of spatial resolution and temperature sensitivity of the X-ray instrument. These small ETBs may significantly contribute to coronal heating.

Acknowledgements This work was supported by the National Natural Science Foundation of China (NSFC, Grant Nos. 10873038 and 10833007), the National Basic Research Program of China (2006CB806302), and CAS Project KJCX2-YW-T04. *Hinode* is a Japanese mission developed and launched by ISAS/JAXA, with NAOJ as the domestic partner and NASA and STFC (UK) as international partners. It is operated by these agencies in cooperation with ESA and the NSC (Norway). The open data policy of the TRACE team is acknowledged.

References

Berghmans, D., Clette, F., & Moses, D. 1998, A&A, 336, 1039
Berghmans, D., & Clette, F. 1999, Sol. Phys., 186, 207
Berghmans, D., Clette, F., Robbrecht, E., & McKenzie, D. 1999, ESASP, 448, 575
Berghmans, D., McKenzie, D., & Clette, F. 2001, A&A, 369, 291
Delaboudiniére, J.-P., Artzner, G. E., Brunaud, J., et al. 1995, Sol. Phys., 162, 291
Domingo, V., Fleck, B., & Poland, A. I. 1995, Sol. Phys., 162, 1
Golub, L., Krieger, A. S., Silk, J. K., et al. 1974, ApJ, 189, L93
Golub, L., Deluca, E., Austin, G., et al. 2007, Sol. Phys., 243, 63
Handy, B. N., Acton, L. W., Kankelborg, C. C., et al. 1999, Sol. Phys., 187, 229
Li, H., Sakurai, T., Ichimito, K., et al. 2007, PASJ, 59, S643
Ogawara, Y., Takano, T., Kato, T., et al. 1991, Sol. Phys., 136, 1
Shimizu, T., Tsuneta, S., Acton, L. W., et al. 1992, PASJ, 44, L147
Shimizu, T., Tsuneta, S., Acton, L. W., et al. 1994, ApJ, 422, 906
Shimizu, T. 1995, PASJ, 47, 251
Shimizu, T. 2004, in Multi-Wavelength Investigations of Solar Activity, eds. A. V. Stepanoov, E. E. Benevolenskaya, & A. G. Kosovichev (Cambridge: Cambridge Univ. Press), 233, 345
Shimizu, T., Katsukawa, Y., Matsuzaki, K., et al. 2007, PASJ, 59, S845
Tsuneta, S., Acton, L., Bruner, M., et al. 1991, Sol. Phys., 136, 37
Zhang, J., Kundu, M. R., & White, S. M. 2001, Sol. Phys., 198, 347